frontiers in Energy Research

ORIGINAL RESEARCH
published: 15 March 2022
doi: 10.3389/fenrg.2022.843518

Evaluation Model and Application of Shale Oil Production Efficiency Under Energy-Depleted Development Mode in Jimsar Sag

Yang Gao[1,2], Dongming Zhi[3], Yingyan Li[2], Zhenxue Jiang[1], Yuan Deng[2] and Jianhua Qin[2]*

[1]Unconventional Oil and Gas Science and Technology Research Institute, China University of Petroleum, Beijing, China, [2]Exploration and Development Research Institute, PetroChina Xinjiang Oilfield Company, Karamay, China, [3]PetroChina Tuha Oilfield Company, Turfan-Hami, China

OPEN ACCESS

Edited by:
Kaiqiang Zhang,
Imperial College London,
United Kingdom

Reviewed by:
Sen Wang,
China University of Petroleum,
Huadong, China
Qingbang Meng,
China University of Geosciences
Wuhan, China

***Correspondence:**
Yang Gao
93446812@qq.com

Specialty section:
This article was submitted to Advanced Clean Fuel Technologies, a section of the journal Frontiers in Energy Research

Received: *10 January 2022*
Accepted: *24 February 2022*
Published: *15 March 2022*

Citation:
Gao Y, Zhi D, Li Y, Jiang Z, Deng Y and Qin J (2022) Evaluation Model and Application of Shale Oil Production Efficiency Under Energy-Depleted Development Mode in Jimsar Sag. Front. Energy Res. 10:843518. doi: 10.3389/fenrg.2022.843518

In order to reveal the shale oil production mechanism and production efficiency under the energy-depleted development mode, experiments on expulsion oil based on imbibition and elastic energy release under high temperature and pressure were carried out, and nuclear magnetic resonance on-line monitoring was used to observe the production characteristics of shale oil. The experimental results show that the imbibition-expulsion oil mainly occurs in the small-size pore-throat system. Under the condition of high temperature and pressure, the oil-expulsion efficiency is generally less than 2% affected by pore pressure, which is significantly different from the conventional imbibition experiment results. Although elastic-energy expulsion oil occurs in different sizes of pore-throat systems, the oil-expulsion efficiency in large size pore-throat systems is more sensitive to temperature. Overall, the total elastic-energy oil-expulsion efficiency is significantly positively correlated with reservoir physical properties, production differential pressure and temperature, and negatively correlated with crude oil viscosity. Comprehensively considering various geological factors affecting oil-expulsion efficiency, the shale oil production efficiency evaluation model under the energy-depleted development mode is constructed, and the movable oil porosity of shale oil development section in the study area is evaluated. The results show that there is a good positive correlation between movable oil porosity and oil production intensity. The movable oil porosity of dry layer is generally lower than 0.5% and that of poor oil layer is between 0.5% and 1.5%. When the movable oil porosity is between 1.5 and 2.5%, it can be determined as the type II oil layer, and for more than 2.5%, it is the type I oil layer. The single-well evaluation results show that the shale oil "sweet spots" of the Lucaogou Formation in Jimsar Sag are mainly distributed in $P_2l_2^{2-1}$~ $P_2l_2^{2-3}$ and $P_2l_1^{2-1}$~ $P_2l_1^{2-3}$, which is in good agreement with the current development status.

Keywords: energy-depleted development, imbibition, elastic-energy, high temperature and pressure, oil production efficiency, shale oil, Jimsar Sag

INTRODUCTION

China is rich in shale oil resources and has stepped from the stage of finding "sweet spot" to developing "sweet spot". At present, shale oil development in China is mostly aimed at medium–high maturity shale, the energy depletion development mode under the volume fracturing technology of horizontal wells has made breakthroughs in Junggar, Bohai Bay, Songliao, Ordos, and other basins (Fu et al., 2019; Mu et al., 2019; Gao et al., 2020; Yang et al., 2020; Zhao et al., 2020). Technically, the development of medium–high mature shale oil is feasible, but its economic benefits are restricted by factors such as oil price, construction cost, and single-well productivity, which is closely related to the resource abundance and crude oil mobility. Therefore, carrying out the shale oil mobility research, clarifying the production mechanism, and establishing the evaluation model of shale oil production efficiency are significant for shale oil development interval optimization and productivity evaluation.

Many scholars have devoted time on the study of shale oil/tight oil mobility based on extraction and pyrolysis (Zhu et al., 2019), whose basic idea is to explain the mobility of shale oil by characterizing the content of free oil. However, the change of temperature and pressure under geological conditions will affect the occurrence state of crude oil, and the accuracy of laboratory experimental results remains to be discussed. Moreover, the free oil content always is regarded as the maximum amount of movable oil, and the actual recovery ratio is much lower than this value. Based on supercritical CO_2 displacement method, Feng et al. (2019) characterized the movable efficiency and movable lower limit of tight oil and clarified the relationship between movable oil rate and reservoir physical properties. This method represents the maximum amount of crude oil that can be recovered in tight reservoir by existing technologies, but it cannot be carried out on a large scale due to the production cost constraints. In addition, digital cores were established to explore the seepage law of fluid in tiny spaces by many foreign scholars (Passey et al., 2010; Desbois et al., 2011; Iglauer et al., 2013; Hemes et al., 2015), but due to the strong heterogeneity of unconventional reservoirs, the digital core model is suffered from the problem of under-representation, so it is also difficult to popularize and apply.

At present, energy depletion exploitation based on hydraulic fracturing is the main development mode of tight oil/shale oil. Theoretically, there are two main oil expulsion mechanisms in the development process of this mode: 1) oil expulsion by imbibition displacement between fracturing fluid and crude oil in matrix pores; 2) oil expulsion by fluid expansion energy in matrix pores. Up to now, many scholars have carried out simulation experiments of different oil displacement mechanisms to clarify the production efficiency. For example, some scholars have conducted imbibition experiments to reveal the effects of oil-expulsion efficiency by reservoir physical properties, fluid concentration difference, and interfacial tension (Cuiec et al.,1994; Wang et al.,2012; Muhammed et al., 2014; Alexeyev, 2017). However, these experiments were carried out under atmospheric pressure and without considering the effect of pore pressure on oil-expulsion efficiency. Ma et al. (2016) carried out oil expulsion experiments of different samples by fluid elastic expansion energy and characterized the differences of oil-expulsion efficiency under different reservoir physical properties and bottom-hole pressure. But the study did not consider the effect of temperature on crude oil mobility nor did it establish an evaluation model of oil-expulsion efficiency regarding physical properties, differential pressure, and other factors.

Considering the current production mode and the expulsion mechanism of shale oil under high temperature and pressure, taking the Lucaogou Formation of Jimsar Sag in the Junggar Basin as an example, this study carried out the imbibition-expulsion oil simulation experiment and energy depletion oil drainage experiments under different temperature and pressure and implemented on-line monitoring by nuclear magnetic resonance (NMR). Based on the experimental results, this study further reveals the production characteristics of shale oil under the hydraulic fracturing: energy depletion development mode, clarifies its influencing factors, and establishes a quantitative evaluation model of shale oil mobility efficiency. The research results not only provide a basis for shale reservoir identification, classification, and productivity evaluation in this area but also provide reference and guidance for the later CO_2 energy enhancement development.

SAMPLES AND EXPERIMENTS

Sample Information and Experimental Environment

Seven samples in this experiment are from the Lucaogou Formation of four wells in Jimsar Sag. Their lithology is siltstone and dolomitic siltstone, which are the main lithology of shale oil reservoir in this area. The porosity of the sample ranges from 7.36 to 19.69%, the permeability ranges from 0.02 mD to 1.009 mD, and the oil-bearing grade ranges from oil stains to saturated oil (**Table 1**). The experimental oil is the actual crude oil of the Lucaogou Formation, with density of 0.85 g/cm^3 at 25°C and viscosity of 110 mPa·s at 55°C.

The experiments were mainly completed on the displacement equipment MR-dd with high temperature and pressure system, and the experimental process was monitored on-line by NMR (MesoMR23-060H I). NMR parameters were set to TE = 0.2 ms, TW = 3000 ms, NECH = 12,000, and NS = 32. The environment temperature was 25°C and the humidity is 30%.

Experimental Steps

This study mainly carries out the simulation experiment of imbibition-expulsion oil and elastic-energy expulsion oil under high temperature and pressure. The experimental device is shown in **Figure 1**, and the process is as follows:

Experiment 1: The simulation experiment of imbibition-expulsion oil under high temperature and pressure: 1) Clean and dry the standard plunger sample of 2.5 cm × 5 cm and measure the nuclear magnetic signal T_2 spectrum. 2) Saturate the vacuumed sample with crude oil at 20 MPa and 60°C for 24 h. 3) Place the sample in the clamp holder and set the

TABLE 1 | Basic information of experimental samples.

No.	Well	Layer	Depth /m	Porosity /%	Permeability /mD	Oil-bearing grade	Lithology
#12	J10012	$P_2l_2^{2-3}$	3177.03	7.36	0.082	Oil stains	Siltstone
#21	J10005	$P_2l_1^{2-2}$	2813.56	13.61	0.045	Oil stains–oil spot	Siltstone
#27	J10025	$P_2l_1^{2-2}$	3699.8	19.69	0.63	Oil saturated	Siltstone
#41	J10024	$P_2l_2^{2-2}$	3482.2	13.03	1.009	Oil spot	Siltstone
#13	J10012	$P_2l_1^{2-3}$	3311.71	15.57	0.02	Oil immersion	Dolomitic siltstone
#31	J10025	$P_2l_1^{2-3}$	3706.22	8.89	0.069	Oil stains–oil spot	Dolomitic siltstone
#38	J10025	$P_2l_1^{2-3}$	3707.78	10.49	0.379	Oil saturated	Dolomitic siltstone

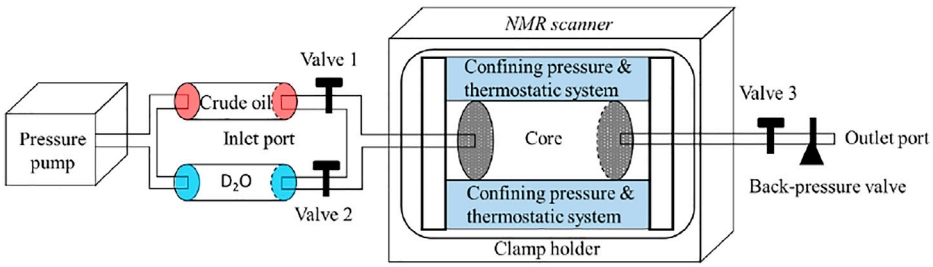

FIGURE 1 | Diagrammatic representation of the experimental device.

experimental temperature at 90°C and the confining pressure at 37 Mpa. Close valves 2 and 3, open valve 1, and fill crude oil with 35 MPa to supplement pore pressure. 4) Close valve 1 when the NMR signal is stable. 5) Open valve 2, fill D_2O at 37 MPa, and start the oil imbibition-expulsion simulation experiment under high temperature and pressure. Monitor the hydrogen signal of crude oil in the core based on NMR at certain intervals; the experiment ends until the NMR signal does not change.

Experiment 2: The simulation experiment of elastic-energy expulsion oil under different temperatures: 1) Cleane, dry, vacuum, and saturate the sample with crude oil. 2) Put the saturated oil sample in the holder and set the experiment temperature to 20°C. Close outlet 2 and 3, open valve 1, and fill crude oil to pore pressure of 35 Mpa. 3) Close valve 1 and open the outlet valve 3 and carry out the elastic-energy expulsion oil simulation experiment under the pressure difference of 35 Mpa. When the NMR signal is stable, the experiment ends. 4) Change the experiment temperature (35°C, 55°C, 75°C, and 90°C), and repeat steps 1~3 to carry out the elastic-energy expulsion oil experiment at different temperatures.

Experiment 3: The simulation experiment of elastic-energy expulsion oil under different pressure: 1) Pretreat the sample as above, set the experiment temperature to 90°C, close valves 1 and 2, open valve 1, and fill crude oil to pore pressure of 35 Mpa. 2) Close valve 1 and set the outlet back-pressure valve to 32 Mpa when the NMR signal is stable. Open valve 3 and allow the sample to expulse oil at a pressure difference of 3 Mpa. 3) Repeat the abovementioned steps, set the pressure of the back-pressure valve to be 30 Mpa, 25 Mpa, 15 Mpa, 5 Mpa, and 0 Mpa, respectively, and carry out the elastic-energy expulsion oil experiment under the different production pressure.

EXPERIMENTAL RESULTS AND ANALYSIS

Imbibition-Expulsion Oil Experiments Under High Temperature and Pressure

In the process of imbibition-expulsion oil, water is imbibed from the fracture into the oil-bearing matrix under the action of capillary force, and the pore with water wetting drives out the crude oil through oil–water replacement (Zhu et al., 2002; Li et al., 2007). In total, four samples were subjected to the imbibition-expulsion oil experiments under high temperature and pressure in this study. The oil-expulsion efficiency is the ratio of the difference between the original saturated oil signal and the residual oil signal to the original saturated oil signal. The experimental results are shown in **Figure 2**.

From the experimental results, the effect of imbibition-expulsion oil under high temperature and pressure is not obvious. The oil expulsion phenomenon occurred only 60 h ago, and the final oil-expulsion efficiency is only 1.4–1.8% (**Figure 2A**). The oil-expulsion efficiency of different samples showed a significant negative correlation with the permeability of unit pore [Log (K)/φ] (**Figure 2B**). It reflects that the pore-throat system with a smaller size has larger capillary force, and it is more likely to have an imbibition-expulsion oil effect. Microscopically, NMR T_2 spectrum also show that the crude oil signal decreases gradually with the imbibition time in the low T_2 area (**Figure 3**), which also intuitively shows that the imbibition phenomenon mainly occurs in the small pore-throat system.

Different from the atmospheric pressure imbibition, when the matrix pore fluid is in a high-pressure state, the imbibition fluid is not only subjected to the capillary power to the matrix pore but also subjected to the outward expansion resistance of

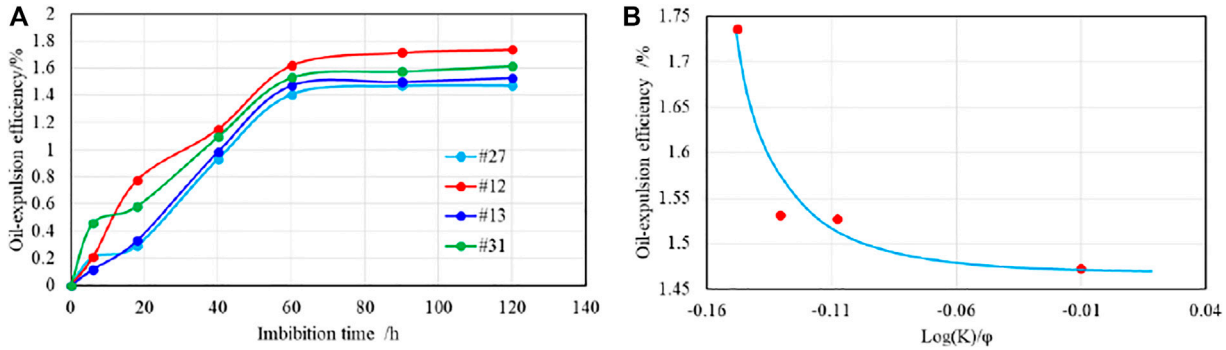

FIGURE 2 | Variation characteristics of imbibition oil-expulsion efficiency. **(A)** Relationship between oil-expulsion efficiency and imbibition time; **(B)** relationship between oil-expulsion efficiency and reservoir physical property.

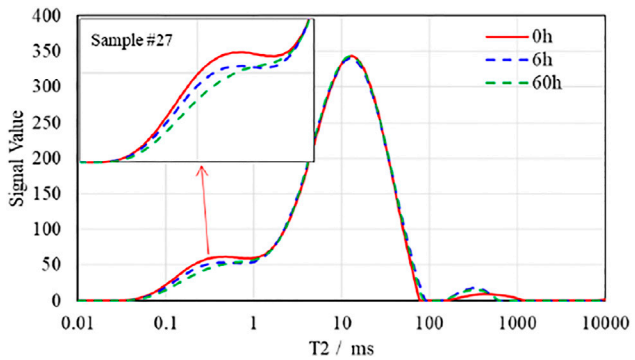

FIGURE 3 | Results of imbibition–NMR experiments under high temperature and pressure conditions.

crude oil in the pore, which greatly reduces the efficiency of imbibition-expulsion oil. The author compared the results of imbibition-expulsion oil under high and atmospheric pressure. The crude oil signal of sample #12 decreased from 5926 to 5364 after 60 h under atmospheric pressure, and the oil-expulsion efficiency could reach about 10%, which was much higher than that under high pressure (**Figure 4**). It can also be confirmed that the existence of pore pressure will counteract the capillary force and prevent the occurrence of imbibition-expulsion oil. In this experiment, D_2O is used as the imbibition fluid. However, in the actual production process, the imbibition fluid is polymer fracturing fluid containing guar gum, and its percolation capacity is much lower than that of D_2O. Therefore, in the actual fracturing and soaking process, the efficiency of imbibition-expulsion oil may be even lower.

Experiment on Elastic-Energy Expulsion Oil at Different Temperature

Under the condition of 35 MPa pore pressure, temperature has a significant effect on the oil-expulsion efficiency of elastic energy, which is mainly reflected in the oil-expulsion of large pores. Also taking #27 as an example, the amount of elastic-energy expulsion oil was less at 20°C, and the total NMR signal decreased from 12,848 to 12,270, corresponding to the oil-expulsion efficiency of 4.5%. As the temperature rose to 55°C, the total oil-expulsion efficiency reached 11.4%, and the oil expulsion mainly occurred in the region of T_2>10 ms (**Figure 5A**). With the further increase of temperature, the NMR signal in high T_2 area gradually decreases and the oil-

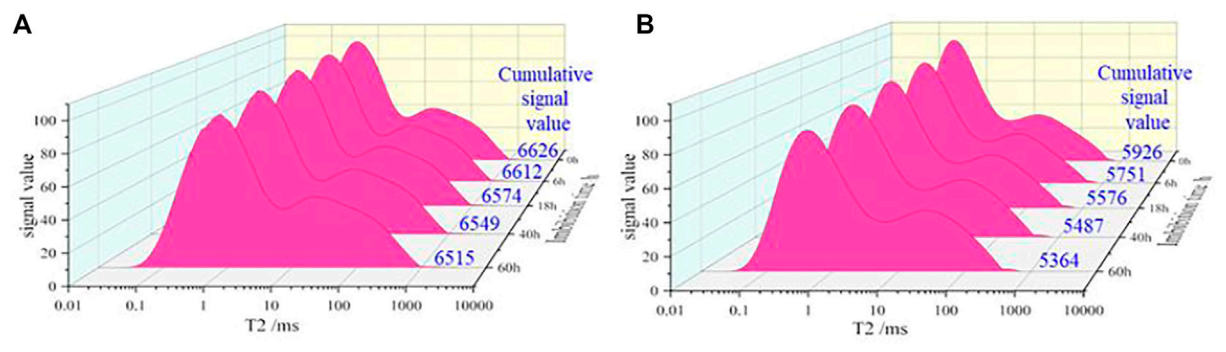

FIGURE 4 | Comparison of imbibition under high **(A)** and atmospheric **(B)** pressure.

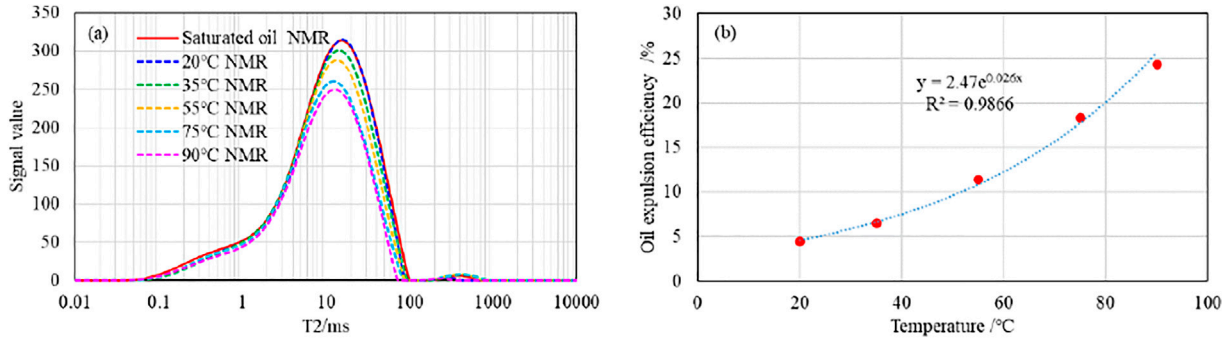

FIGURE 5 | NMR T_2 spectrum after elastic-energy expulsion oil at different temperatures **(A)** and relationship between temperature and oil-expulsion efficiency **(B)**.

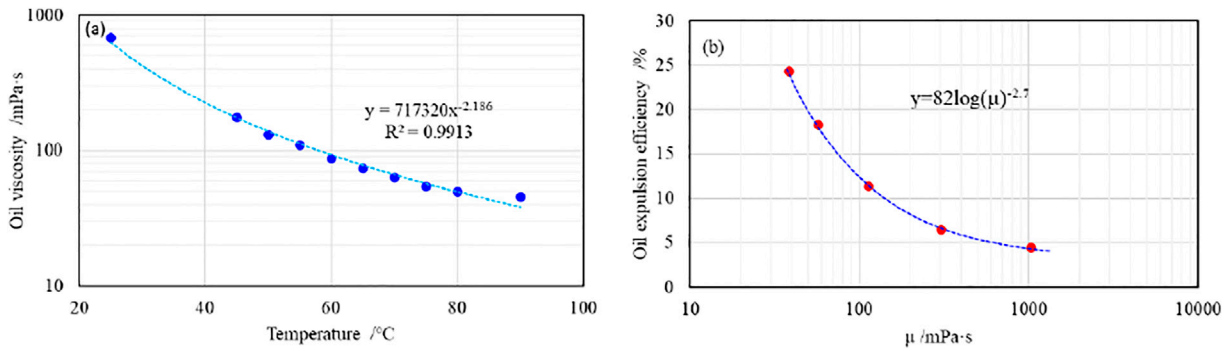

FIGURE 6 | Variation of crude oil viscosity with temperature **(A)** and the effect of viscosity on the oil-expulsion efficiency **(B)**.

expulsion efficiency further increased, reaching 24.4% at 90°C (**Figure 5B**).

In the elastic-energy expulsion oil stage, the driving force of oil-expulsion is the expansion energy of the fluid, which can be reflected as the fluid pressure within the matrix pores. The expulsion resistance is mainly the capillary force of the reservoir and the viscous force of the crude oil. With the same reservoir properties and pore pressure, the increase of temperature essentially reduces the crude oil viscosity (μ) and changes the viscous force of the crude oil, so as to improve the production efficiency of crude oil in matrix pores. The author measured the experimental oil viscosity at different temperatures, which presented a power function negative correlation (**Figure 6A**). It can be seen that with increase in temperature and decrease in crude oil viscosity, the expulsion efficiency of crude oil increases rapidly. Especially when the viscosity is below 100 mPa s, the improvement rate of oil-expulsion efficiency is further intensified (**Figure 6B**).

Experiment on Elastic-Energy Expulsion Oil at Different Differential Pressure

The elastic-energy oil expulsion experiments of seven samples were carried out at 90°C and different differential pressures (3 Mpa, 5 MPa, 10 MPa, 20 MPa, 30 MPa, and 35 MPa). There is a good linear positive correlation between the NMR signal of saturated oil sample and gas porosity (**Figure 7**), indicating that the sample has a high degree of saturation and meets the experimental requirements. The NMR data of the experimental samples at saturated oil state and after oil expulsion state are shown in **Table 2**.

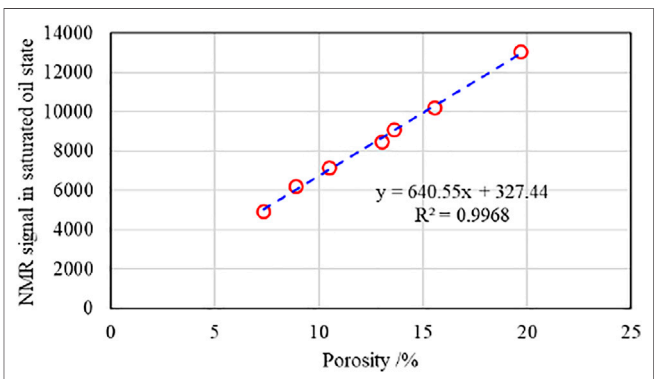

FIGURE 7 | Relationship between the NMR signal and gas porosity at the saturated oil state.

TABLE 2 | NMR data of the experimental samples at the saturated oil state and after the oil expulsion state.

Sample	NMR signal after oil expulsion at different differential pressure						
	Saturated	3 MPa	5 MPa	10 MPa	20 MPa	30 MPa	35 MPa
#41	8461	8124	7725	7316	6953	6554	6256
#27	13054	11900	11700	11287	10631	10110	9719
#21	9078	8591	8376	8097	7743	7410	7074
#12	4928	4717	4635	4568	4474	4321	4222
#38	7156	6909	6683	6414	6117	5859	5478
#31	6218	6062	5749	5581	5357	5227	5191
#13	10178	9847	9522	9328	9013	8724	8443

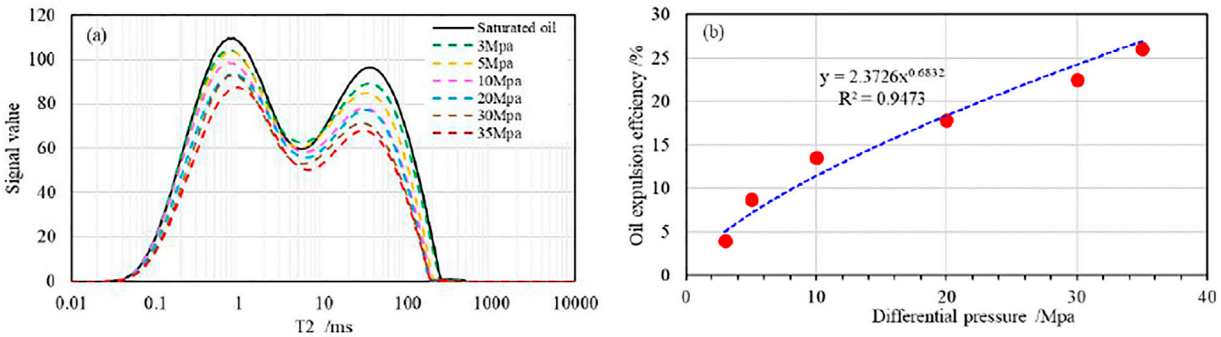

FIGURE 8 | NMR T_2 spectrum of elastic-energy oil expulsion under different differential pressure **(A)** and variation characteristics of oil-expulsion efficiency with differential pressure **(B)**.

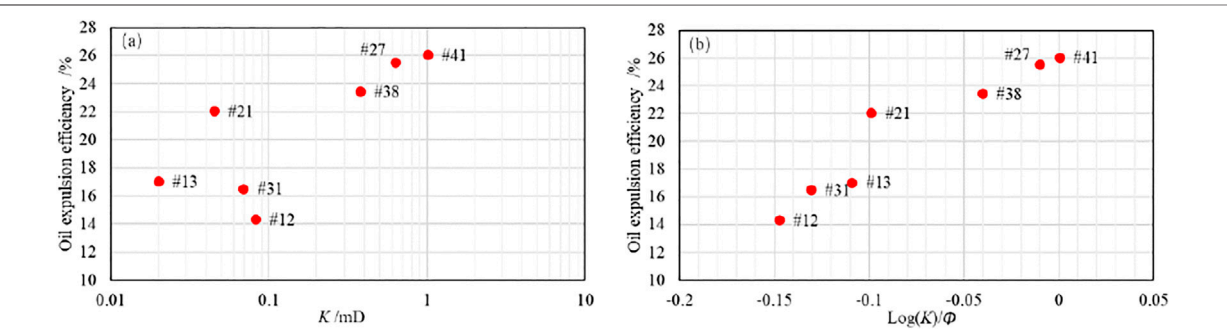

FIGURE 9 | Relationship between reservoir physical properties and oil-expulsion efficiency at differential pressure of 35 MPa.

Taking sample #41 as an example, the NMR T_2 spectrum shows bimodal characteristics, and the pore-throat size distribution ranges widely. With the increase of pressure difference, the NMR signal of crude oil in different size pores gradually decreases, which shows that crude oil is discharged from pores with different sizes (**Figure 8A**). As the production differential pressure rises from 5 to 35 MPa, the oil-expulsion efficiency increases from 4% to 26% in a power function (**Figure 8B**).

With the same fluid properties and production pressure difference, the oil-expulsion efficiency is mainly affected by the reservoir physical properties, especially the permeability (Huang et al., 2019). It is true that the high permeability of the reservoir is indeed conducive to the discharge of crude oil from the matrix pores, but in the process of elastic-energy oil expulsion, the pore volume and fluid elastic modulus are also the key factors restricting the oil-expulsion efficiency. **Figure 9A** shows that permeability is an important but not the only factor controlling oil-expulsion efficiency. For example, samples #12 and #31 have higher permeability than samples #13, but their oil-expulsion efficiency is lower due to their low porosity. Therefore, the pore-throat structure parameter Log $(K)/\Phi$ is constructed, which has a good positive correlation with elastic-energy oil-expulsion efficiency (**Figure 9B**).

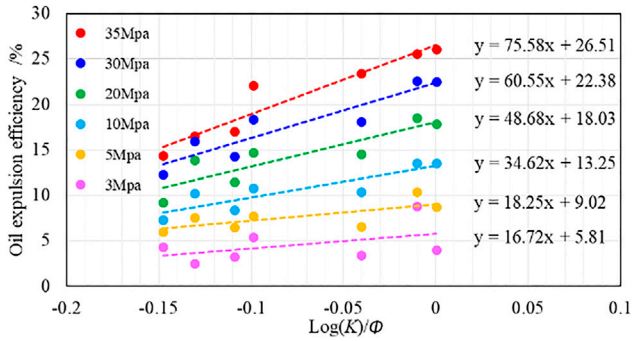

FIGURE 10 | Characteristics of elastic-energy oil-expulsion efficiency of samples with different physical properties under different pressure differences.

DISCUSSION

Evaluation Model of Shale Oil Production Efficiency Under Energy-Depleted Development Mode

The relationship between oil-expulsion efficiency and Log $(K)/\Phi$ of seven samples shows that they are linear under the same differential pressure (**Figure 10**). The general expression is $y = Ax + B$, and its characteristic performance parameters A and B increase with the increase of differential pressure (**Figure 10**).

Since there is a significant linear relationship between parameters A and B ($B = 0.37A$) (**Figure 11A**), the oil-expulsion efficiency with respect to the reservoir structure coefficient can be expressed as follows:

$$E_o = A \times \left(\mathrm{Log}(K)/\Phi + 0.37\right). \quad (1)$$

Here E_o is the oil-expulsion efficiency, %; K is permeability, mD; and Φ is porosity, %.

Due to the same experimental temperature and experimental oil, parameter A should be a variable controlled by differential pressure. The relationship between parameter A and differential pressure reveals that they have a good power function relationship (**Figure 11B**), so **Eq. 1** can be further expressed as follows:

$$E_o = 7.74\Delta\mathrm{Pa}^{0.62} \times \left(\mathrm{Log}(K)/\Phi + 0.37\right), \quad (2)$$

where ΔPa represent the fluid differential pressure, MPa; Other parameters are the same as before.

According to **Eq. 2**, the oil-expulsion efficiency is negative when Log $(K)/\Phi$ is less than −0.37, which is obviously inconsistent with the fact. But it also reveals the lower physical property limit of elastic-energy expulsion oil, that is, Log $(K)/\Phi$ = −0.37. When the physical property is lower than this value, the oil-expulsion efficiency is 0.

In addition to fluid differential pressure and reservoir physical properties, temperature also has significant impact on shale oil-expulsion efficiency, which is manifested in the impact of temperature on oil viscosity. The elastic-energy expulsion oil experiment of sample #27 at different temperatures reveals that the oil-expulsion efficiency is negatively correlated with the logarithm of crude oil viscosity in a power function, which can be expressed as follows:

$$E_o = 82 \times \mathrm{Log}(\mu)^{-2.7}, \quad (3)$$

where μ represent the viscosity of crude oil, Mpa; Other parameters are the same as before.

Therefore, considering the crude oil viscosity, fluid pressure difference, and reservoir physical properties, the oil-expulsion efficiency under the energy-depleted development mode can be expressed as follows:

$$E_o = C \times \mathrm{Log}(\mu)^{-2.7} \times \Delta\mathrm{Pa}^{0.62} \times \left(\mathrm{Log}(K)/\Phi + 0.37\right), \quad (4)$$

where C represent a comprehensive constant, dimensionless; Other parameters are the same as before.

Sample #27 has a porosity of 19.7% and a permeability of 0.63 mD; when the production differential pressure is 35 Mpa, the expression of $\Delta\mathrm{Pa}^{0.62} \times$ [Log $(K)/\Phi$+0.37] in **Eq. 4** is equal to 3.26. Thus, the **Eq. 4** can be expressed as follows:

$$E_o = 3.26\, C \times \mathrm{log}(\mu)^{-2.7}. \quad (5)$$

Eq. 3, **Eq. 5** are equal, so the comprehensive constant C is 25.2. Under the energy-depleted development mode, the evaluation model of shale oil production efficiency of the Lucaogou Formation in Jimsar Sag is expressed as follows:

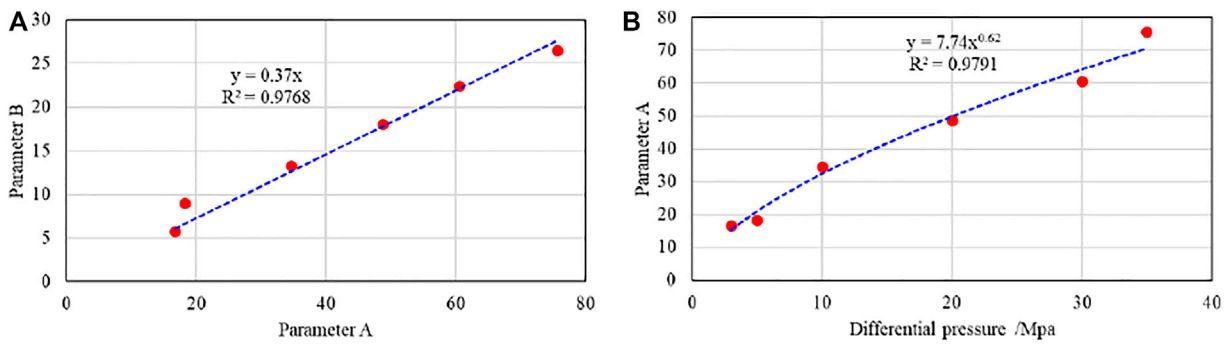

FIGURE 11 | Relationship between parameters A and B **(A)**, and relationship between parameter A and differential pressure **(B)**.

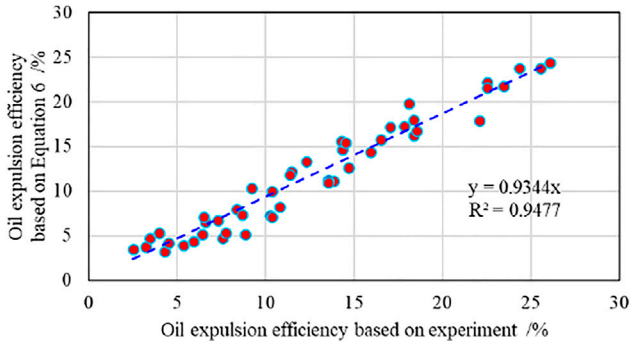

FIGURE 12 | Comparison of oil-expulsion efficiency between experiment and model evaluation.

$$E_o = 25.2\times \mathrm{Log}(\mu)^{-2.7}\times \Delta \mathrm{Pa}^{0.62}\times(\mathrm{Log}(K)/\Phi + 0.37). \quad (6)$$

According to **Eq. 6**, the energy-depleted oil-expulsion efficiency of the experimental samples at different temperatures and different differential pressure are calculated. The evaluation results are in good agreement with the experimental results, and the correlation coefficient R^2 is as high as 0.95 (**Figure 12**).

Evaluation and Application of Shale Oil Energy-Depleted Production Efficiency

From a geological point of view, the single-well productivity of shale oil is controlled by the physical properties, oil content, and movable efficiency of the reservoir. NMR logging has unique advantages in reservoir evaluation, which can effectively evaluate the porosity, permeability, and oil saturation of the reservoir. Wang et al. (2019) combined experimental measurement results and NMR relaxation time of bound-water of different types of clay and determined the starting NMR time of effective porosity of shale oil reservoir of the Lucaogou Formation in Jimusar is 1.7 ms. Xiao et al. (2013) and Chen et al. (2017) considered the strong heterogeneity of tight reservoir and quantitatively classified the reservoir according to the flow unit index (FZI) from small to large using NMR logging data. The porosity and permeability of each type of flow unit have good correlation, so the permeability can be evaluated according to NMR porosity. Based on the simulation experiment and nuclear magnetic logging, Mao and Shen (2021) and Yan et al. (2021), respectively, used 1D and 2D NMR logging to realize the quantitative evaluation of oil saturation of tight reservoir/shale reservoir.

The current geothermal gradient of the Lucaogou Formation in Jimsar Sag is about 3.1°C/hm and the formation pressure coefficient is around 1.36. Based on the relationship between temperature and crude oil viscosity (**Figure 6A**), as well as the difference between formation pressure and bottom-hole pressure, the shale oil production efficiency of the target formation has been evaluated combined with the porosity and permeability calculated by the above method. The evaluation parameter movable oil porosity (Φ_{om}), which integrates reservoir physical properties, oil-bearing properties and mobility ($\Phi_{om} = \Phi \times S_o \times E_o$), was further constructed, and the quantitative evaluation of this parameter was carried out for the target interval. The results show that there is a good positive correlation between Φ_{om} and oil production intensity in the perforated interval of a single well (**Figure 13**). According to the oil production conclusion, the Φ_{om} of dry layer is basically lower than 0.5%, that of poor oil layer is between 0.5%–1.5%, and that of oil layer is greater than 1.5%. Further, according to the productivity difference of oil layers, the oil layer with $\Phi_{om} > 2.5\%$ is determined as type I oil layer, and the oil layer with $\Phi_{om} = 1.5$–2.5% is determined as type II oil layer (**Figure 13**).

Application results of reservoir classification and evaluation method reveal that, type I and II shale oil layers of Lucaogou Formation are mainly distributed in $P_2l_2^{2-1}$~ $P_2l_2^{2-3}$, and $P_2l_1^{2-1}$~ $P_2l_1^{2-3}$, which are the upper and lower shale oil "sweet spot" sections in Jimsar Sag (**Figure 14**). The lithology of the "sweet spot" section is mainly feldspathic-lithic siltstone and dolomitic sandstone. Under the syn-quasi-synthetic leaching and organic acid dissolution, the reservoir performance is effectively improved (Wang et al., 2020), providing a large amount of storage space for shale oil in the "sweet spot" section. The sections of $P_2l_2^{2-4}$ and $P_2l_1^{2-4}$~ $P_2l_1^{2-7}$ corresponds to the lacustrine transgressive and high-stand system tracts of third-order sedimentary cycle, developing two sets of high-quality hydrocarbon source rocks (Yang et al., 2018; Zhang et al., 2021). They provide sufficient oil sources for the upper and lower sweet sections, making the oil saturation of the sweet sections average around 70% and locally up to 90%. Based on frozen argon ion polishing SEM, Wang et al. (2021) revealed that the heavy components of crude oil mainly exist in the pores below 300 nm and the pore walls above 300 nm, which are mostly in the adsorbed and bound states and difficult to be used. The light-medium components are mainly stored in the center of pores above 300 nm, which is also the main contributor to the available shale oil. In the feldspathic-lithic siltstone and dolomitic

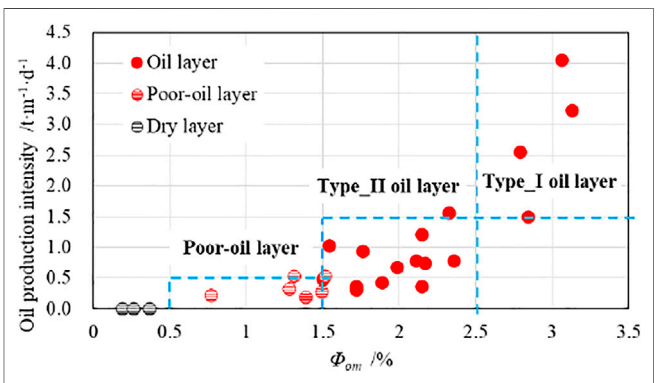

FIGURE 13 | Relationship between Φ_{om} and oil production intensity of the Lucaogou Formation in Jimsar Sag.

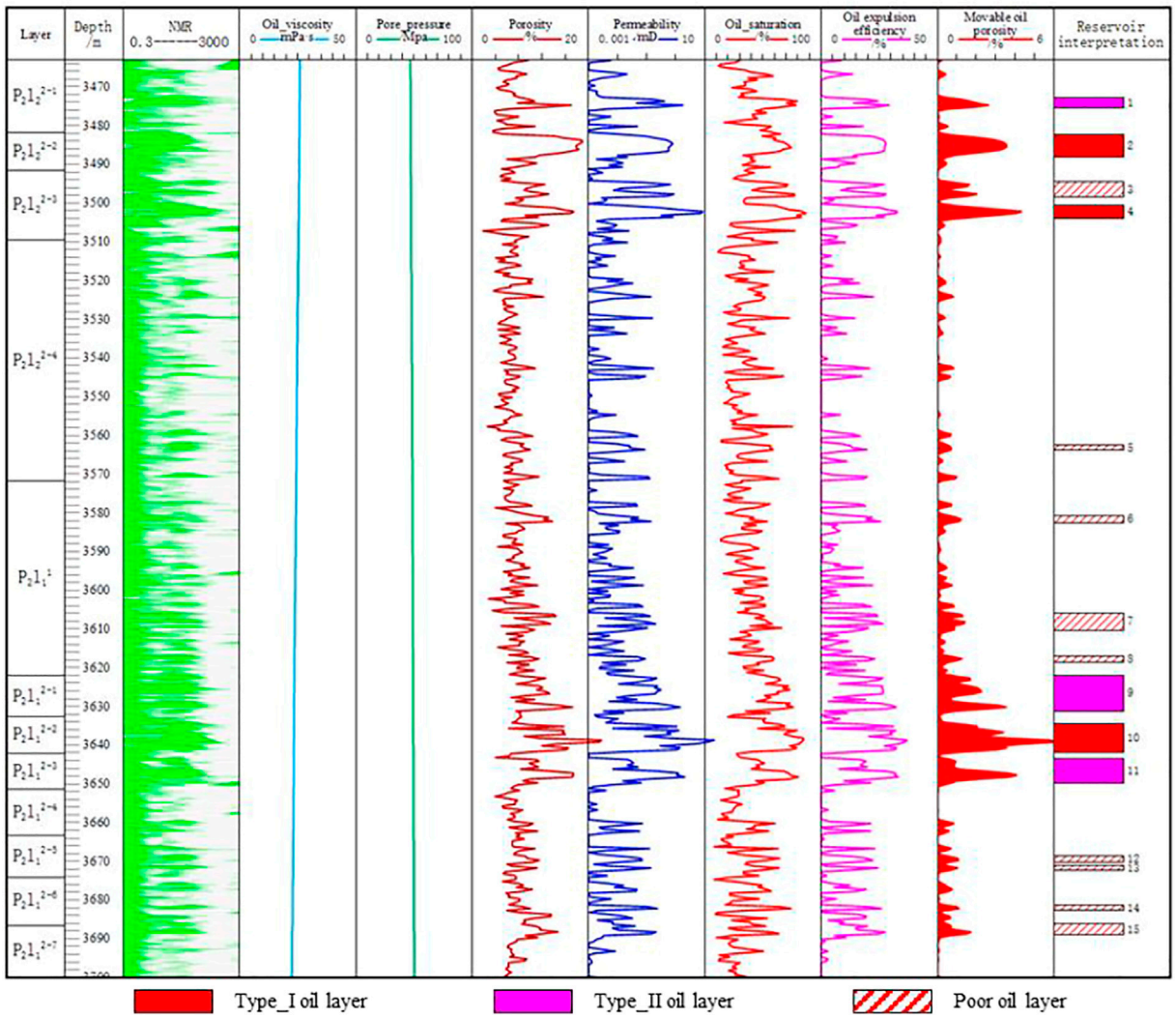

FIGURE 14 | Comprehensive interpretation of shale oil mobility in well J10024.

siltstone of the study area, the pores with size above 300 nm accounts for about 75 and 60% respectively (Wang et al., 2021), which also ensure that the shale oil from the upper and lower "sweet spot" sections has high mobility efficiency.

It can be seen that the upper and lower "sweet spot" sections have superior shale oil enrichment conditions, and the dissolution and expansion porosity effects of the two main lithologies also make the shale oil in these two "sweet spot" sections have good mobility. In addition, the evaluation results based on this study further confirm that $P_2l_2^{2-1}$~ $P_2l_2^{2-3}$ and $P_2l_1^{2-1}$~ $P_2l_1^{2-3}$ have high movable oil porosity and are favorable sections for shale oil development in this area.

CONCLUSION

1) Imbibition-expulsion oil mainly occurs in the small-size pore-throat system and the oil-expulsion efficiency is negatively correlated with the reservoir physical properties. Affected by the fluid pressure in the pores, the imbibition oil-expulsion efficiency of shale oil in the high-pressure formation is not more than 2%, which is far lower than the results of conventional imbibition experiments.
2) Elastic-energy expulsion oil experiment and the model reveal that the oil-expulsion efficiency is positively correlated with production differential pressure and physical properties and negatively correlated with crude oil viscosity. The lower limit of production physical properties is log $(K)/\Phi = -0.37$. The evaluation accuracy of the model is as high as 95%.
3) The sections of $P_2l_2^{2-1}$~ $P_2l_2^{2-3}$ and $P_2l_1^{2-1}$~ $P_2l_1^{2-3}$ in Jimsar Sag have superior geological conditions for shale oil enrichment. The evaluation results show that type I and II oil layers are mainly developed in these sections, which are the mainstay of shale oil development in the area.

DATA AVAILABILITY STATEMENT

The raw data supporting the conclusion of this article will be made available by the authors, without undue reservation.

AUTHOR CONTRIBUTIONS

YG is responsible for research and writing the manuscript. DZ is responsible for technical guidance in the research process. YL is responsible for the application of the model. ZJ is responsible for technical guidance in the research process. YD is responsible for drawing the pictures in the manuscript. JQ is responsible for technical guidance in the research process.

FUNDING

This study was supported by the major projects of CNPC (No. 2019E–2607, 2019E–2608).

REFERENCES

Alexeyev, A. (2017). "Integrated Reservoir Characterization of the Middle Bakken in the Blue Buttes Field, Williston Basin, North Dakota[C]," in//SPE Western Regional Meeting. doi:10.2118/185664-ms

Chen, Z. Q., Wu, S. Y., and Bai, R. (2017). Logging Evaluation for Permeability of Tight sandstone Gas Reservoirs Based on Flow Unit Classification : a Case from Xujiahe Formation in Guang'an Area, central Sichuan Basin [J]. *Lithologic Reservoirs* 29, 76–83. doi:10.3969/j.issn.1673-8926.2017.06.010

Cuiec, L., Bourbiaux, B., and Kalaydjian, F. (1994). Oil Recovery by Imbibition in Low-Permeability Chalk. *Spe Formation Eval.* 9, 200–208. doi:10.2118/20259-PA

Desbois, G., Urai, J. L., Kukla, P. A., Konstanty, J., and Baerle, C. (2011). High-resolution 3D Fabric and Porosity Model in a Tight Gas sandstone Reservoir:A New Approach to Investigate Microstructures from Mm- to Nm-Scale Combining Argon Beam Cross-Sectioning and SEM Imaging. *J. Pet. Sci. Eng.* 78, 243–257. doi:10.1016/j.petrol.2011.06.004

Feng, J., Zhang, B. W., and Feng, Z. H. (2019). Crude Oil Mobility and its Controlling Factors in Tight Sand Reservoirs in Northern Songliao Basin, China. [J]. *Pet. Exploration Dev.* 46, 312–321. doi:10.11698/PED.2019.02.1110.1016/s1876-3804(19)60012-1

Fu, J. H., Niu, X. B., and Dan, W. D. (2019). The Geological Characteristics and the Progress on Exploration and Development of Shale Oil in Chang 7 Member of Mesozoic Yanchang Formation, Ordos Basin. [J]. *China Pet. Exploration* 24, 601–614. doi:10.3969/j.issn.1672-7703.2019.05.007

Gao, Y., Ye, Y. P., and He, J. X. (2020). Development Practice of Continental Shale Oil in Jimsar Sag in the Junggar Basin. [J]. *China Pet. Exploration* 25, 133–141. doi:10.3969/j.issn.1672-7703.2020.02.013

Hemes, S., Desbois, G., Urai, J. L., Schröppel, B., and Schwarz, J.-O. (2015). Multi-scale Characterization of Porosity in Boom Clay (HADES-Level, Mol, Belgium) Using a Combination of X-ray μ-CT, 2D BIB-SEM and FIB-SEM Tomography. *Microporous mesoporous Mater.* 208, 1–20. doi:10.1016/j.micromeso.2015.01.022

Huang, W. B., Zhan, Z. C., and Lu, R. J. (2019). Microscope Dynamic Process and Controlling Factors of Oil Charging in Tight Reservoir [J]. *Oil Gas Geology.* 40, 1197–1204+1214. doi:10.11743/ogg20190604

Iglauer, S., Paluszny, A., and Blunt, M. J. (2013). Simultaneous Oil Recovery and Residual Gas Storage: A Pore-Level Analysis Using *In Situ* X-ray Micro-tomography. *Fuel* 103, 905–914. doi:10.1016/j.fuel.2012.06.094

Li, S. K., Liu, W. D., and Zhang, H. Q. (2007). Experimental Study of Spontaneous Imbibition in Low-Per Meability Reservoir [J]. *Acta Petrolei Sinica* 109-112. doi:10.1016/S1872-5813(07)60034-6

Ma, Q. Z., Yang, S. L., and Lv, D. P. (2016). Study on the Low of Elastic Recovery of Tight Reservoir and its Influence Factors [J]. *Sci. Tech. Eng.* 16, 147–151+156. doi:10.3799/dqkx.2017.609

Mao, R., and Shen, Z. M. (2021). Evaluation Method of Reservoir Oil-Bearing Property by NMR Logging of Permian Lower Wuerhe Formation in Mahu Sag, Junggar Basin [J]. *China Pet. Exploration* 26, 162–172. doi:10.3969/j.issn.1672-7703.2021.04.013

Mu, L. J., Zhao, Z. F., and Li, X. W. (2019). Fracturing Technology of Stimulated Reservoir Volume [J]. *Pet. Nat. Gas Geology.* 40, 626–635. doi:10.11743/ogg20190317

Muhammed, F. A., Bai, B., and Imqam, A. (2014). "SPE-170067-MS Preformed Particle Gel-Enhanced Surfactant Imbibition for Improving Oil Recovery in Fractured Carbonate Reservoirs [C]," in//SPE Heavy Oil Conference-Canada, Calgary, Alberta, Canada, 10-12 June. doi:10.2118/170067-MS

Passey, Q. R., Bohacs, K. M., and Esch, W. L. (2010). "From Oil-Prone Source Rock to Gas-Producing Shale Reservoir–Geologic and Petrophysical Characterization of Unconventional Shale-Gas Reservoirs [C]," in// International oil and gas conference and exhibition in China. OnePetro. doi:10.2118/131350-MS

Wang, D., Seright, R. S., and Zhang, J. (2012). "Wettability Survey in Bakken Shale with Surfactant-Formulation Imbibition [J]," in *Spe Reservoir Evaluation & Engineering.* doi:10.2118/153853-PA

Wang, J., Zhou, L., and Jin, J. (2021). Pore Structure, Hydrocarbon Occurrence and Their Relationship with Shale Oil Production in Lucaogou Formation of Jimsar Sag, Junggar Basin. [J]. *Pet. Geology. Exp.* 43, 941–948. doi:10.11781/sysydz202106941

Wang, R., Chang, Q. S., and Qian, Y. X. (2020). Reservoir Characteristics and Genesis of Shale Oil "Sweet Spots" in Lucaogou Formation, Jimsar Sag, Junggar Basin [J]. *Pet. Geology. Exp.* 42, 604–611. doi:10.11781/sysydz202004604

Wang, W., Zhao, Y. W., and Mao, R. (2019). Determination of the Starting Time for Measurement of NMR Effective Porosity in Shale Oil Reservoir: A Case Study of the Permian Lucaogou Shale Oil Reservoir, Jimusaer Sag [J]. *Oil Gas Geology.* 40, 550–557. doi:10.11743/ogg20190310

Xiao, L., Liu, X.-p., Mao, Z.-q., Zou, C.-c., Hu, X.-x., and Jin, Y. (2013). Tight-Gas-Sand Permeability Estimation from Nuclear-Magnetic-Resonance (NMR) Logs Based on the Hydraulic-Flow-Unit (HFU) Approach. *J. Can. Pet. Tech.* 52, 306–314. doi:10.2118/167255-pa

Yan, W. L., Zhang, Z. Q., and Chen, L. C. (2021). New Evaluating Method of Oil Saturation in Gulong Shale Based on NMR Technique [J]. *Pet. Geology. Oilfield Dev. Daqing.* 40, 78–86. doi:10.19597/J.ISSN.1000-3754.202107007

Yang, J. G., Li, S. C., and Yao, Y. L. (2020). Significant Breakthrough in the Continental Shale Oil Survey in Northern Songliao Basin. [J]. *Geology. Resour.* 29, 300. doi:10.3969/j.issn.1671-1947.2020.03.015

Yang, Z., Hou, L. H., and Lin, S. H. (2018). Geologic Characteristics and Exploration Potential of Tight Oil and Shale Oil in Lucaogou Formation in Jimsar Sag [J]. *China Pet. Exploration* 23, 76–85. doi:10.3969/j.issn.1672-7703.2018.04.009

Zhang, Y. F., Zha, M., and Ding, X. J. (2021). Evaluation and Controlling Factors of Shale Oil Bearing Properties of Permian Lucaogou Formation in Jimsar Depression [J]. *Xinjiang Geology.* 39, 297–301. doi:10.3969/j.issn.1000-8845.2021.02.016

Zhao, W., Hu, S., Hou, L., Yang, T., Li, X., Guo, B., et al. (2020). Types and Resource Potential of continental Shale Oil in China and its Boundary with Tight Oil. *Pet. Exploration Dev.* 47, 1–11. doi:10.1016/S1876-3804(20)60001-5

Zhu, W. Y., Ju, Y., and Zhao, M. (2002). Spontaneous Imbibition Mechanism of Flow through Porous media and Water Flooding in Low-Permeability

Fractured sandstone Reservoir [J]. *Acta Petrolei Sinica* 56-59+3. doi:10.3321/j.issn:0253-2697.2002.06.012

Zhu, X. M., Zhu, W. B., and Cao, J. (2019). Research Progress on Shale Oil Mobility Characterization [J]. *Xinjiang Pet. Geology.* 40, 745–753. doi:10.7657/XJPG20190617

Conflict of Interest: YG, YL, YD, and YG were employed by the PetroChina Xinjiang Oilfield Company. DZ was employed by the PetroChina Tuha Oilfield Company.

The remaining author declares that the research was conducted in the absence of any commercial or financial relationships that could be construed as a potential conflict of interest.

Publisher's Note: All claims expressed in this article are solely those of the authors and do not necessarily represent those of their affiliated organizations, or those of the publisher, the editors, and the reviewers. Any product that may be evaluated in this article, or claim that may be made by its manufacturer, is not guaranteed or endorsed by the publisher.